Al-Azhar Bulletin of Science

Volume 34 | Issue 2 Article 10

2023
Section: Physics

Electrical and Optical Characteristics of Wide Pressure-Range Capacitive Coupled RF Discharge

Diaa Ibrahim
diaa@eaeat.edu.eg

Abdou Garamoon

Farouk Elakshar

Ashraf Alsharif

How to Cite This Article

Ibrahim, Diaa; Garamoon, Abdou; Elakshar, Farouk; and Alsharif, Ashraf (2023) "Electrical and Optical Characteristics of Wide Pressure-Range Capacitive Coupled RF Discharge," *Al-Azhar Bulletin of Science*: Vol. 34: Iss. 2, Article 10.
DOI: https://doi.org/10.58675/2636-3305.1645

ORIGINAL ARTICLE

Electrical and Optical Characteristics of Wide Pressure-range Capacitive Coupled RF Discharge

Diaa Ibrahim [a,*], Abdou Garamoon [b], Farouk Elakshar [b], Asharf F. El-sherif [c], Mansour ElSabbagh [b,d]

[a] Egyptian Academy for Engineering and Advanced Technology, Egypt
[b] Physics Department, Faculty of Science, Al-Azhar University, Cairo, Egypt
[c] Head of Electrical Power and Machines Department, College of Engineering Science & Technology, Misr University for Science and Technology (MUST), Giza, Egypt
[d] Center of Plasma Technology, Al-Azhar University, Cairo, Egypt

Abstract

A homemade RF capacitive coupled discharge system operating in wide range of pressures (from low pressure up to atmospheric pressure) was constructed. Electrical and optical characteristics of the constructed system were measured for argon discharge operated at wide range of pressure (from low pressure up to atmospheric pressure) and RF power up to 150 Watt. The discharge was operated using two bare metallic copper electrodes with separation distance of 5 mm and it was kept constant in all discharge conditions. Discharge current and discharge voltage were measured for various power and argon gas pressure conditions. The electrical characteristics of the discharge revealed that the discharge is operated in glow mode for all the discharge conditions of the current work. Asymmetric effect was not observed in moderate and high-pressure conditions. Consumed power, phase angle, and plasma impedance were deduced. Optical emission spectra were acquired, and they were used to estimate electron excitation temperature (T_{exc}) using Boltzmann plot method. Rotational (T_{rot}) and vibrational (T_{vib}) temperatures were evaluated by comparing the experimental observation of nitrogen second positive system ($N_2[C^3\Pi_u] \rightarrow N_2[B^3\Pi_g]$) with simulated spectra. Evaluated values of T_{exc}, T_{rot} and T_{vib} proved that the discharge of the current work is nonthermal discharge which is good candidate to deposit different materials from gas phase of discharge operated with different gases.

Keywords: Electrical characteristics, Electron excitation temperature, Optical emission spectroscopy, RF capacitive coupled discharge, Rotational & vibrational temperatures

1. Introduction

Due to their numerous applications like thin-film deposition, etching, and plasma cleaning, Capacitive Coupled radio frequency discharges are widely studied in a variety of pressure ranges, ranging from a few mTorr to atmospheric pressure [1]. Low pressure plasma has various applications in materials processing especially in the production of semiconductor devices. The temperature of the gas is typically less than 150 °C, ensuring that thermally sensitive substrates are not harmed. Ions generated by the plasma can be accelerated toward a substrate, resulting in the directional etching of nano features [2]. Atmospheric-pressure gas discharge plasmas have more benefits in practice than low-pressure gas discharge plasma sources. Lower capital costs for the entire plasma generation and processing system, no size restrictions on the treated materials, more flexible operations, and the costly and complex vacuum system has been removed as a result [1,2]. The atmospheric-pressure glow discharge plasma (APGD) using bare metallic electrodes driven by radiofrequency (RF)

Received 18 December 2022; revised 8 March 2023; accepted 11 March 2023.
Available online 23 November 2023

* Corresponding author at: Egyptian Academy for Engineering and Advanced Technology, Cairo, Egypt. Fax: +(202) 265 787 0.
E-mail address: diaa@eaeat.edu.eg (D. Ibrahim).

https://doi.org/10.58675/2636-3305.1645

power supply which is called RF APGD has developed in recent years and attracted much attention from researchers in the world [1]. In the literature, there are two types of RF APGD. The first type is RF APGD using two metallic bare electrodes and the second type is RF APGD using dielectric material between the two electrodes. The first type gives a homogeneous discharge, and it has a lower discharge voltage compared with the second type [2]. Most of RF APGD sources are employing helium as a carrier gas. But when argon tries to take the place of helium as a carrier gas to drastically cut operating costs associated with gas use, problems with its ignition and maintaining stability, as well as its constrained chemical and physical operation windows when reactive gas (like O_2 or N_2) is added, become acute. Therefore, the argon capacitive APGD operated by RF power supply at atmospheric pressure is given a lot of attention to increase its performance [3,4]. However, the majority of the authors concentrate on low or atmospheric pressure with little work in the range from moderate to atmospheric [5]. Capacitively coupled plasma (CCP) systems can be divided according to the geometry of the two electrodes into symmetric discharge when includes two identical electrodes area whilst asymmetric when plasma formed between two unequal electrode areas at low pressure produces a dc voltage as a result of differences in electron and ion mobility, Due to this bias, the smaller electrode experiences high sheath voltages and high ion energies [6]. RF APGD plasma may thus be used in a larger range of applications, like, deposition, decontamination of chemical and biological warfare agents, water treatment, safety, etching, etc, and even create new applications [7]. One of these applications is to synthesis a graphene oxide (GO) using plasma-assisted reaction and deposition at low temperatures [8,9]. A large scale of GO can be produced by preparation of a single layer of graphene and then using oxygen plasma to generate GO.

GO is mainly synthesized by low pressure ICP discharge [10,11]. And by a microwave atmospheric pressure plasma jet [12].

In the current work, we designed and built a homemade RF capacitively coupled RF plasma source operated with bare metallic electrodes (having a separation distance of 5 mm) to generate argon plasma at a wide pressure range (from 25 mbar up to 1 bar) with the intention to use it in synthesizing a graphene oxide using argon and methane gases mixture. The electrical and the optical characteristics of the built source were studied for different RF power and gas pressure.

2. Experiment setup

The experimental setup is shown in Fig. 1, the discharge was produced between two circular copper metallic electrodes. The upper electrode was one centimeter in diameter cooled by water and the lower electrode was six centimeters in diameter. The upper electrode is connected to the RF power supply (13.56 MHz) via a homemade π type matching network and the lower electrode was connected to the ground. The matching network was made of an inductor and two variable air-gap capacitors. The reflected power was minimized by tuning the capacitors of the matching network. Both electrodes were enclosed in a stainless-steel vacuum chamber and the chamber was connected to the ground. The gap between the two electrodes was fixed at 5 mm. The discharge voltage was measured using a homemade Resistor–Capacitive voltage probe (1:24) and the discharge current was measured using a commercial current probe (Pearson Current Monitor 2877). A GWINSTEK digital oscilloscope (model GDS2000) was used to record the voltage and the current waveforms. The optical emission spectroscopy (OES) at the discharge region was monitored using a UV–VIS Avantes spectrometer. The base pressure which was mainly air, was fixed at 1.3 torr and an argon gas is flowed in the chamber to the desired pressure. It should be mentioned here that, all the argon gas pressures used in the current study are a mixture of argon gas and air with the ratio of pressure minus base pressure to the base pressure.

3. Result and discussion

3.1. Electrical characteristics

The electrical characteristics of the discharge system were studied by measuring the discharge voltage and the discharge current waveforms for a wide range of argon gas pressure and consumed RF power. Figure 2 shows the current–voltage waveforms at different pressures. It is noticed that both current and voltage waveforms are close to be sinusoidal at low pressure and they became sinusoidal with increasing the pressure. The current lead the voltage at all conditions which indicates that the discharge type is capacitive coupled plasma (CCP). The current is smoother than the voltage and hasn't any spike. The asymmetric effect cannot be seen in moderate and high pressure as shown in Fig. 2b–d, on the other hand, the effect of asymmetric discharge can be observed clearly in the voltage waveform at a pressure 3.5 mbar as can be seen in Fig. 2a. Because

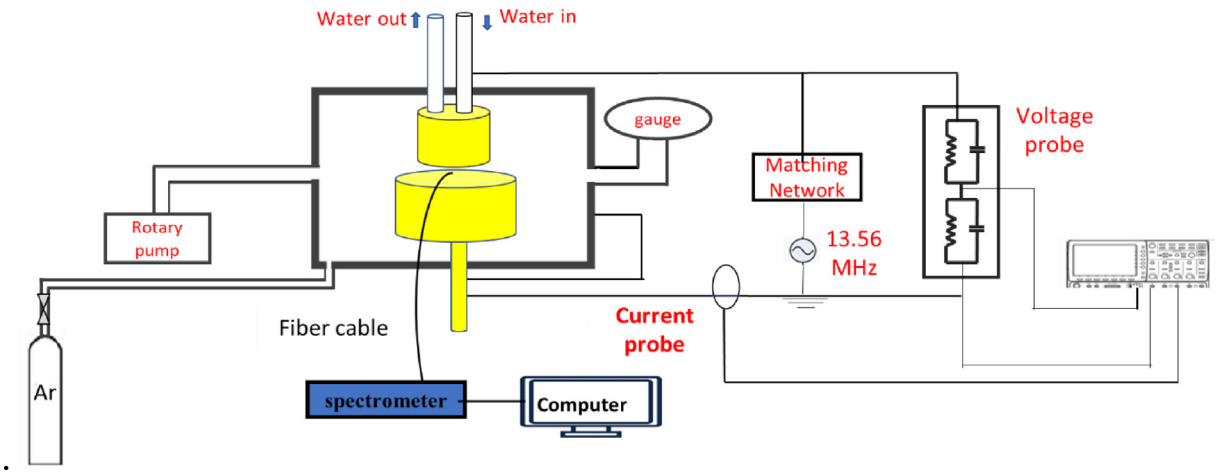

Fig. 1. Schematic diagram of the experimental setup.

the discharge is always in the midplane between the two electrodes in moderate and high pressure, the effect of asymmetric is not seen in the waveform; however, in low pressure, the discharge occupies the entire chamber and asymmetric discharge is visible clearly [13]. A fast Fourier transform was calculated for the discharge voltage for argon gas pressure of 3.5 mbar and 0.8 bar and it is shown in Fig. 3. At argon pressure of 0.8 bar, the amplitude of the third and fifth harmonics of the voltage waveforms are around 1 % and 4 % of the main frequency respectively but at 3.5 mbar, the second, third, fourth, and fifth harmonics are around 3 %, 5 %, 4 % and 1% respectively.

Figure 4 shows the root mean square value of voltage (V_{rms}) against the root mean square value of the current (I_{rms}) for argon discharge generated at different input RF power and pressure. Figure 4a is depicted for moderate & low argon pressure (3.5 mbar–30 mbar) while Fig. 4b is depicted for high argon pressure (0.2 bar–0.8 bar). In the range of 0.2–0.8 bar the discharge voltage increases by increasing the argon pressure at constant discharge current which indicates that the discharge impedance increases with increasing the discharge voltage. The voltage at 0.8 bar starts at 120 V and decreases to 100 V and stays almost unchanged. The current at low pressure is larger than that at moderate and high pressure which might be ascribed to the increase of both of electron density and electron temperature with decreasing the gas pressure. Where with increasing the gas pressure, the electron

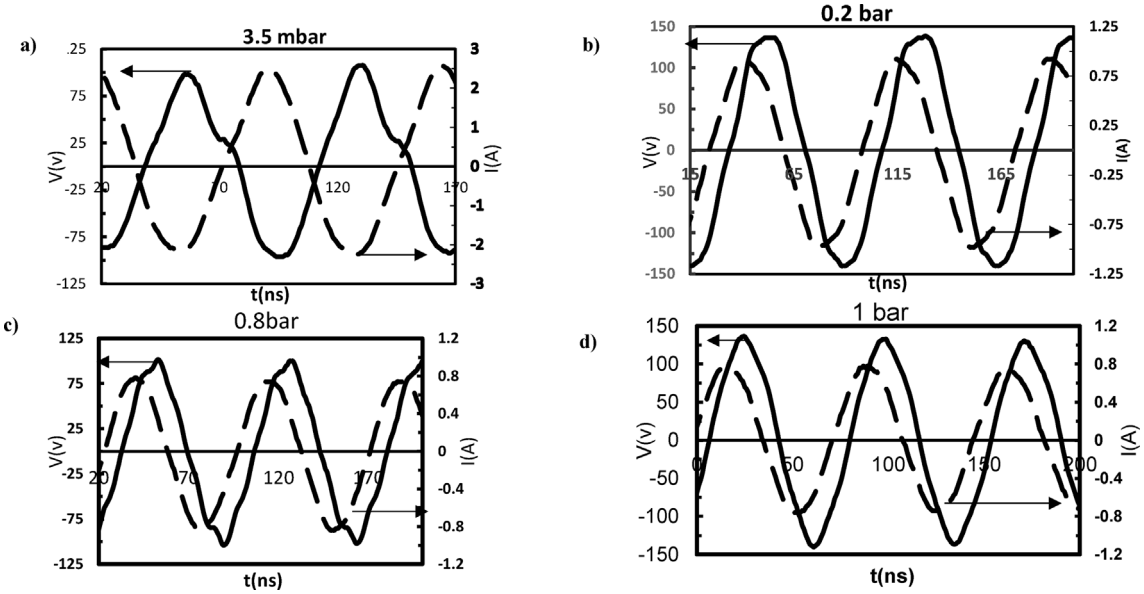

Fig. 2. Current-voltage waveforms of argon discharge at different pressure.

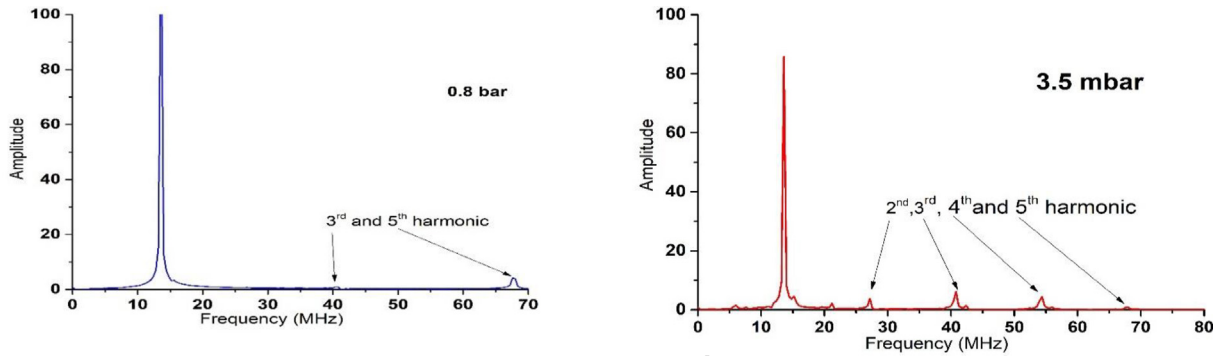

Fig. 3. Fast Fourier transform for voltage at 0.8 bar and 3.5 mbar.

mean free path is decreasing and the electrons will gain less energy from the electric field between successive collisions. This implies that the electron temperature will decrease and as a result the ionization will decrease too. For all discharge conditions shown in Fig. 4, the discharge voltage remains constant with increasing discharge current which indicates that the discharge is operating in normal glow mode for the whole pressure range used in the current work [8].

Dissipated power in the discharge P, discharge impedance Z and phase between the discharge voltage and discharge current waveforms can be estimated by the following equations [14]:

$$P = I_{rms}\, V_{rms} \cos\theta \tag{1}$$

$$Z = \frac{V_{rms}}{I_{rms}} \tag{2}$$

$$\theta = 2\times\pi\times f\times\Delta t \tag{3}$$

Where V_{rms} and I_{rms} are the RMS value of the discharge voltage and the discharge current, is the phase difference between them, is the frequency and is the time shift.

The consumed power calculated from equation 1 as a function of input power for different argon pressure is shown in Fig. 5. The consumed power changes linearly with the input power and it was found that it was about 40–50 % of the delivered power by the RF source. Due to 'The maximum power theorem principle' the maximum power transfer to the discharge cannot be higher than 50 % of the input power that happens when the impedance of the matching network matched with the load impedance [15].

The current–voltage phase angle was less than 90° as shown in Fig. 6 and it was decreasing by increasing the input power which indicated that the plasma became more resistive. The phase angle was never reached zero at all pressures used in the experiment. As a result, the capacitive element in the rf plasma generated in our experiment was always significant. These results suggest that the discharge is not an arc plasma in low, moderate, and high pressure, because arc plasmas are more resistive and their current waveform deviates significantly from sinusoidal [16]. For argon pressures of 25 and 30 mbar and for high RF power, the phase angle is less than 10°. This shows that the discharge shows more resistive in these pressure and powers.

Figure 7 shows the relation between the input power and impedance at argon pressure of 0.2 bar. It is noted that the impedance is linearly decrease

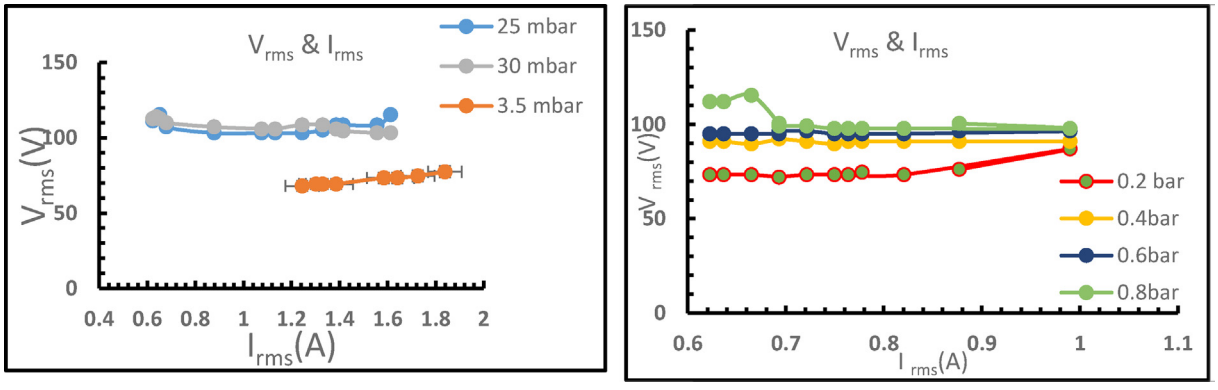

Fig. 4. The root mean square (RMS) value of voltage and current at different pressure.

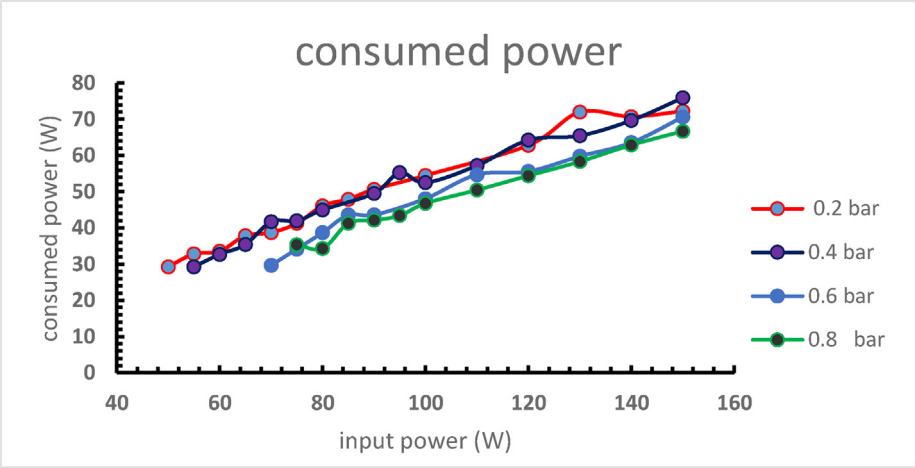

Fig. 5. Consumed power as a function of input power at different pressure.

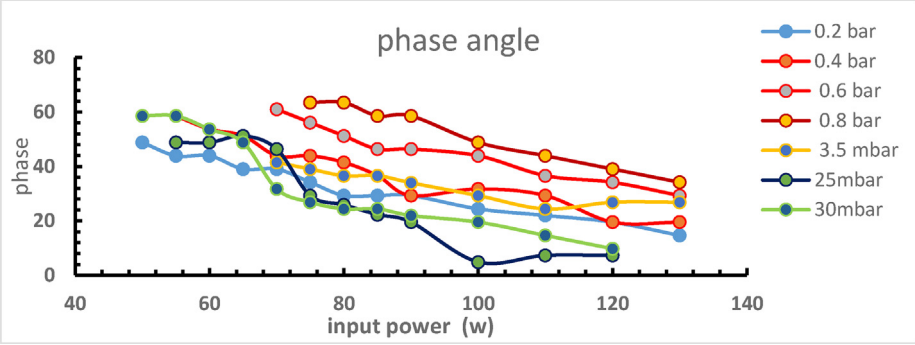

Fig. 6. Phase angle as a function of the input power.

with increasing the input power. This is expected since the degrees of ionization of the discharges of argon increases as the discharge current increases and the discharge voltage stay almost unchanged resulting in a decrease in the impedance of the discharge. Similar results were reported before in argon and nitrogen discharges [7].

Figure 8a & b shows a series of Lissajous figures of voltage–current at different RF power for argon pressure of 30 mbar & 0.2 bar respectively. It is noticed that the area of the figures decreases as the input power increase due to the decreasing of the phase angle between the current and voltage signals. The plot also shows distortions, as opposed at

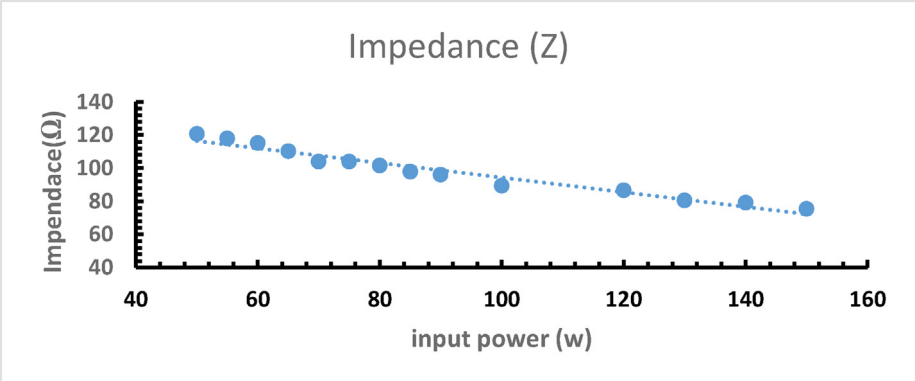

Fig. 7. Plasma impedance as a function of input power at argon pressure of 0.2 bar.

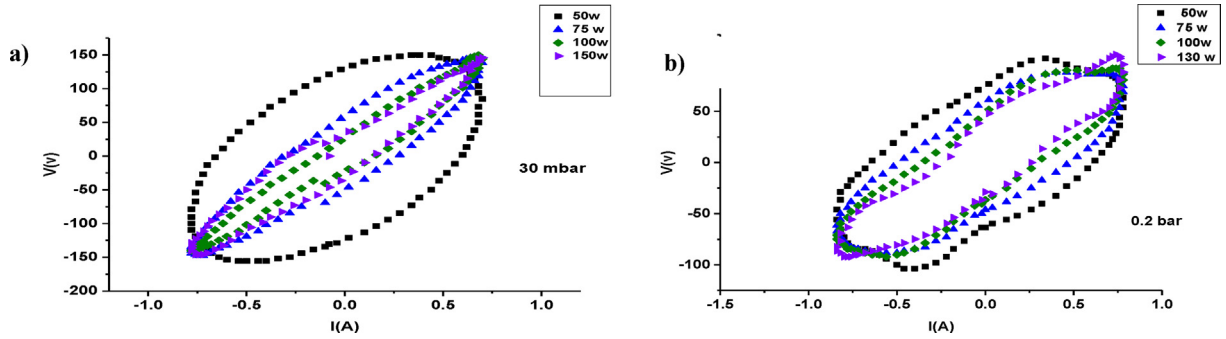

Fig. 8. Lissajous figures of voltage–current at different RF power.

0.2 bar to the smooth profile seen in the case at 30 mbar. The dissertation in the Lissajous pattern is due to the higher conductivity of the discharge, at high power where the discharge becomes more resistive [17].

3.2. Visualization of the discharge

Figure 9 shows photographs of the discharge at different pressure and for RF power of 100 Watt at a constant gap. It is noted that with increasing the argon pressure, the discharge be more localized between the two electrodes. At low pressure (25 mbar) the discharge is faint and covers the two electrodes. For discharge at argon pressure of 0.2 bar, clear discharge regions are observed where shiny positive column is sheen which covers the whole electrodes area. The positive column radius is clearly decrease with increasing the argon pressure. The discharge channel between the electrodes becomes narrower and narrower with increasing the argon pressure from 0.6 bar to 1 bar. Positive column can be seen clearly at the middle between the electrodes. The bright layer on the electrodes can be seen in the region from 0.4 to 1 bar. At 0.8 and 1 bar the discharge usually moves between the electrodes. Symmetric discharge pattern is seen at region 0.6–1 bar with a bright negative glow near the electrodes and a weak positive column in the middle. The maximum emitted light's intensity is so near to the electrodes that the distance between them cannot be calculated [18]. The presence of a pure ɣ mode of an RF discharge is shown by comparing the discharge pattern to the literature for medium-pressure discharges. This type of emission profile was observed before not only in high-pressure discharges [19] but also in moderate pressure discharges [20]. γ-Mode of RF capacitively coupled discharge is a discharge in which electron avalanche is mainly due to the emission secondary electron from the electrode surface by ion bombardment.

3.3. Optical emission

Optical emission was also measured at different pressure using Avantes spectrometer. Figure 10 shows the spectrum at 0.2 bar and 1 bar for an input power of 150 W. Optical emission spectra can be classified into three regions UV, VIS, and IR.

3.3.1. UV region

UV regions are shown in Fig. 11 for 0.2 bar and 1 bar. It is noted that the emission of nitrogen 2nd positive system is seen clearly in a range from 350 to 400 nm ($N_2[C^3\Pi_u] \rightarrow N_2[B^3\Pi_g]$ emission bands, with emission (0,1) band head at 357.8 nm, emission (2,4) band head at 370.7 nm, emission (1,3) band head at 375.2 nm emission (0,2) band head at 380.3 nm, emission (2,5) band head 394.1 nm, and emission (1,4) band head 399.5 nm. This emission is attributed to the presence of residual air in the chamber [21].

3.3.2. Visible region

N_2 second positive system of Nitrogen is also seen in the visible region from 400 to 700 nm. Emission (0,

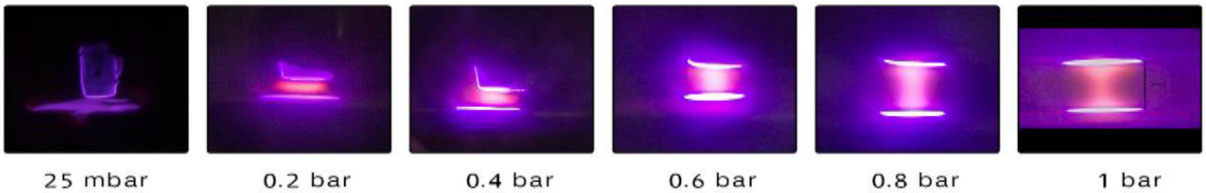

Fig. 9. Photographs of the discharge at different pressure.

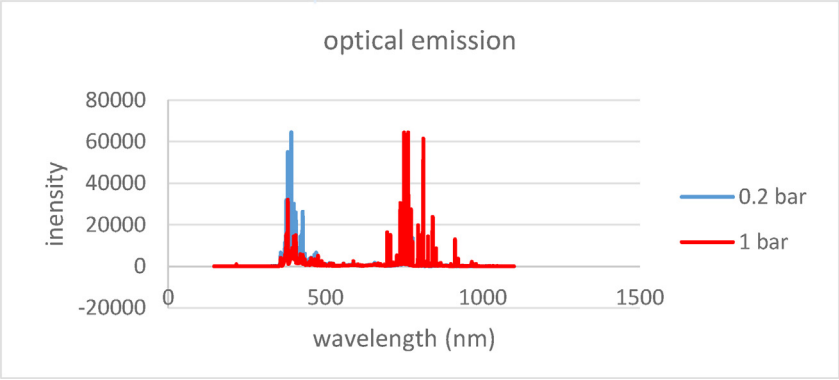

Fig. 10. Optical emission of argon discharge at 0.2 bar and 1 bar.

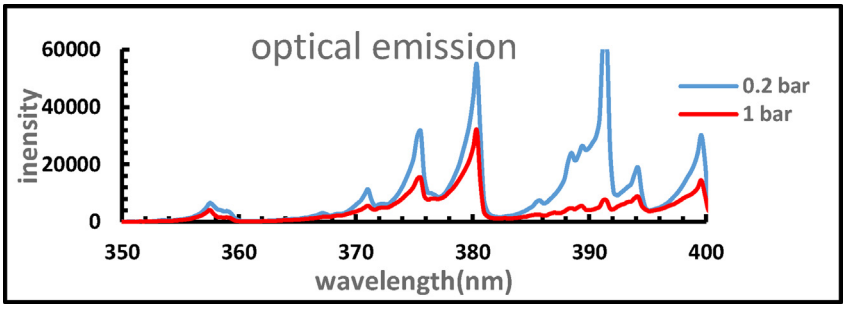

Fig. 11. Emission of 2nd positive system of Nitrogen in argon discharge at RF power of 150 Watt.

3) band head at 405.5 nm, emission (4, 8) band head at 4.9.4 nm, emission (2, 6) band head at 419.9 nm, and emission (1, 5) band head at 427.7 nm. Lines of atomic and ionic argon are also existed, as can be seen in Fig. 12 and Table 1.

3.3.3. Near IR

Strong argon lines and atomics oxygen were observed in the region from 700 to 950 nm as shown in Fig. 13. Oxygen lines of 777 nm and 844 nm were found in the spectrum due to the residual air in the chamber. For all the discharge conditions in the current study it was noted that the emission intensity of the argon lines increases with the increasing discharge pressure while the emission intensity of the nitrogen second positive system decreases with increasing discharge pressure.

3.4. Excitation temperature

The electronic excitation temperature T_{exct} is determined by fitting a thermal distribution to the appropriately weighted intensities of a set of atomic transitions for a specific atomic species in the plasma [22]. In the case of RF CCP discharge, the atomic species used is Argon (Ar). The emitted Argon atoms are excited in the plasma and the excited Argon atoms will emit spectra when they are de-excited. The intensity Iij of Ar I atomic emission lines when Ar -atoms are de-excited from an initial

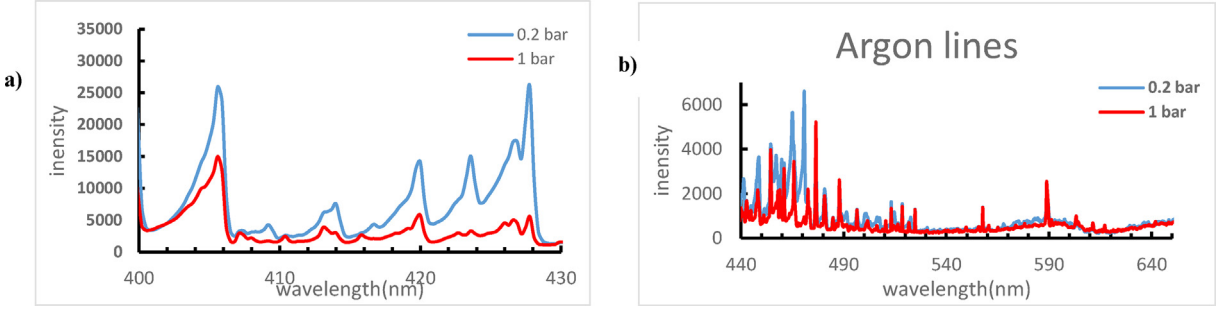

Fig. 12. (a) Emission of 2nd positive system of Nitrogen (b) Emission of Argon lines.

Table 1. Lines of atomic and ionic argon.

Wavelength (nm)	Species
441.5	Ar II
448.7	Ar II
454.4	Ar II
460.9	Ar II
465.7	Ar II
476.5	Ar II
480.9	Ar II
488.14	Ar II
513.17	Ar II
518.5	Ar I
527.4	Ar I
557.7	Ar I
588.8	Ar I

excited state i to final state j is given by the following equation.

$$ln\left(I_{ij}\lambda_{ij}/g_iA_{ij}\right) = -\frac{1}{K_BT_{exct}}E_j + C$$

Where λ_{ij} is the wavelength of the emitted line. The plot of $ln(I_{ij}\lambda_{ij}/A_{ij}g_i)$ as a function of E_i for each of selected emitted Ar lines, gives points which would be perfectly aligned in the case of plasma in local thermal equilibrium (LTE). The slope of this line is $-1/T_{exct}$ leading to T_{exct} which is a good approximation for T_e in the case of LTE. This plot is called Boltzmann plot [23] Each observed Ar II line wavelength has an associated energy level E_j, a statistical weight g_i, and atomic transition probability A_{ij} As given in Table 2. In our experiment, we get E_j,g_i, and A_{ij} from the NIST Atomic Spectra Database [24].

Figure 14 shows Boltzmann plot for argon discharge at pressure 0.8 bar and at RF power of 150 Watt. The data was fitted well with a straight line giving T_{exc} of 3.1 eV. Figure 15 shows electron temperature as a function of argon pressure at RF power of 150 Watt calculated from Boltzmann plot. The electron temperature decreases from 3.5 eV to 2.5 eV with increasing the pressure. This can be explained as follows: the mean free path and the energy gained by the electron decrease as the pressure increases, decreasing the ionization process with increasing the pressure, the number of atoms and molecules increases, so instead of the electron gaining energy from the electric field, more and more energy is transferred from electron to plasma species (atoms, molecules.., etc.) during inelastic collisions, the mean free path decreases, the collision rate of electrons with atoms increases, and the electron's acquired energy decreases, resulting in an increase in electron density and a decrease in electron temperature [25].

Table 2. Spectroscopic parameters of selected Ar atomic and ionic emission lines.

E_j(ev)		Wavelength (nm)	intensity	g_i	(s^{-1})
22.51	−23.50513635	441.03	10109.12	6	1.20E+08
21.14	−25.30588416	460.9	14007.3	8	7.89E+07
19.8	−23.83515388	476.50	23916.7	4	6.40E+07
19.8	−23.67225261	454.5	18905.2	4	4.10E+07
19.22	−25.70475244	480.6	6683.9	6	7.80E+07
19.68	−25.14568661	487.8	12152.8	6	8.23E+07

3.5. Rotational and vibrational temperatures

Measuring the plasma temperatures (electron temperature (T_e), vibrational temperature (T_{vib}), rotational temperature (T_{rot}), and gas temperature (T_g) gives access to information concerning the chemical reactivity of the medium and the thermal energy produced. At atmospheric pressure, collisions between the neutral and excited molecules are more effective and T_{rot} tends to equilibrate with the kinetic temperature of the heavy species T_g. T_{vib} is indicative of vibrationally excited species that is chemically reactive. Thus, T_{rot} & T_{vib} are important parameters to consider in any plasma applications. Emission of OH band and bands of N_2 second positive system, are widely used in estimating. T_{rot}

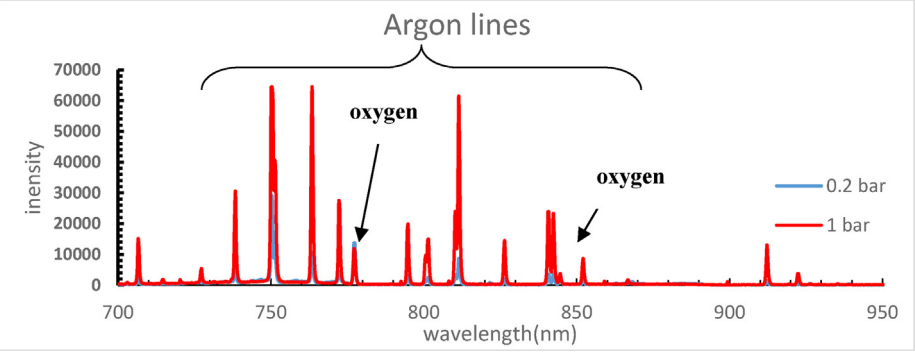

Fig. 13. Emission of argon discharge in region 700–950 nm.

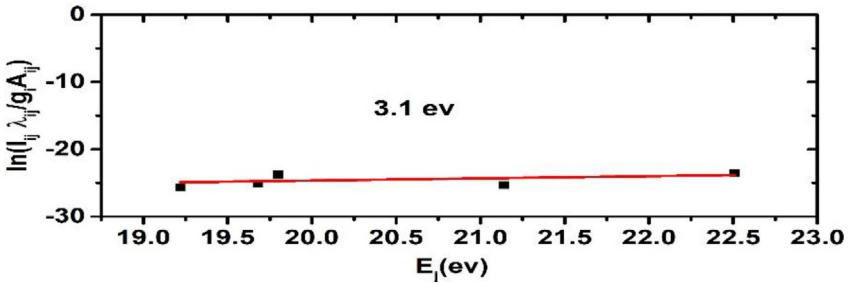

Fig. 14. Boltzmann plot for discharge obtained at argon pressure of 0.8 bar and RF power of 150 Watt.

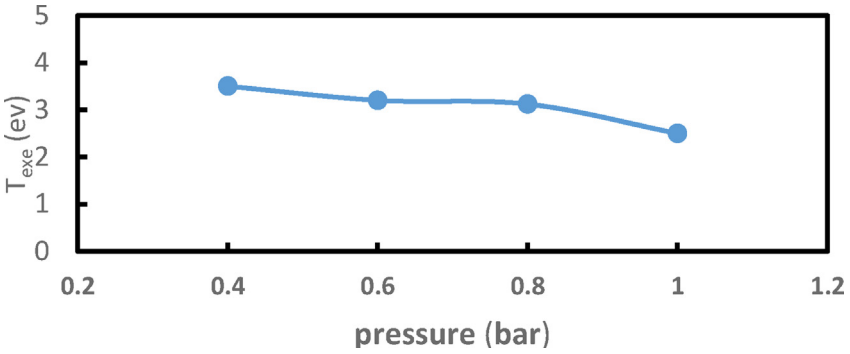

Fig. 15. Electron temperature as a function of argon pressure at RF power of 150 Watt.

& T_{vib} in low-pressure and atmospheric pressure discharges [26]. Among the methods for measuring the rotational and vibrational temperatures the most widely used is that Boltzmann plot. Other methods, however, can be quoted which is based on comparison between experimentally measured lines and normalized theoretically generated curves for different temperatures; this method was adapted in the current research. The emission spectrum of N_2 second positive system due to the transition $C^3\Pi u - B^3\Pi g$ could be obtained with sufficient intensity in nitrogen discharge and in some cases of air discharge. To determine the state vibrational kinetics of the nitrogen molecules in the discharge and to understand vibrational temperature, we measured the relative population density of vibrational excited states of $N_2C^3\Pi u$ with a vibrational quantum numbers $\nu = 0-4$ by emission spectroscopy. As mentioned above that the gas temperature is well approximated with the rotational temperature of N_2 under atmospheric discharge. Rotational and vibrational temperature is obtained from a comparison of N_2 second positive system spectra observed experimentally with simulated ones using software (spectrasim) developed at Technical University of Eindhoven [27].

Figure 16 shows a comparison between experimentally observed spectra of nitrogen second positive system and simulated spectra for discharge generated at argon pressure of 0.8 bar and Rf power of Watt, where T_{rot} & T_{vib} are fitting parameters. From this figure it is clearly seen that there is a nice agreement between the measured and simulated spectra. The best fitting was obtained for T_{rot} of 1645 K and T_{vib} of 3500 K. The dependence T_{rot} & T_{vib} deduced from nitrogen second positive system on argon pressure is shown in Fig. 17. From Fig. 17, it can be seen that T_{rot} is less than T_{vib} for all pressure conditions used in the current study. Both of T_{rot} & T_{vib} are much lower than T_{exc} deduced from Boltzmann plot method in all the work of the

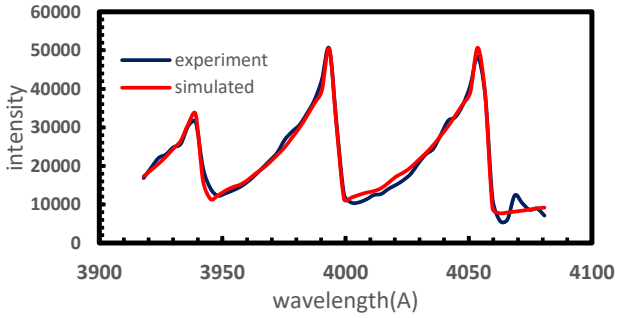

Fig. 16. Comparison of experimental spectrum with simulated one for discharge generated at argon pressure of 0.8 bar and RF power of 150 Watt.

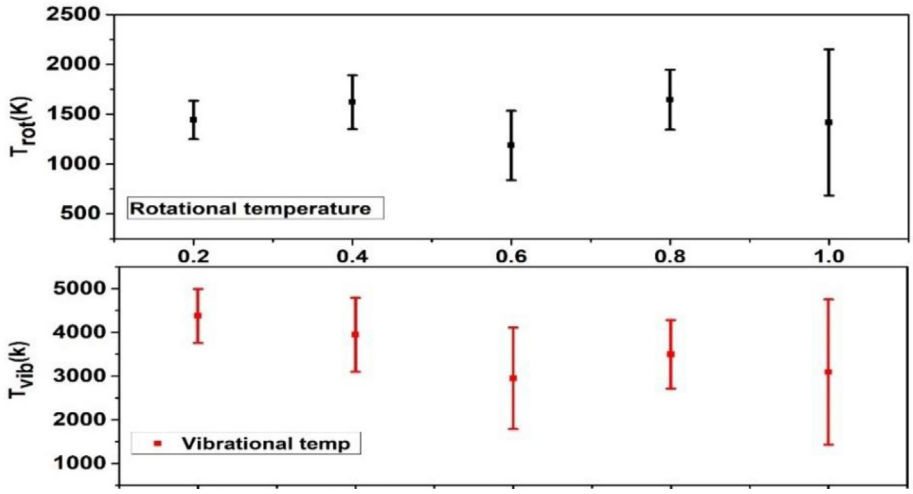

Fig. 17. Pressure dependence of T_{rot} & and T_{vib} where RF power is kept constant at 150 watts.

current study which indicating that the discharge is nonthermal discharge. The nonthermal discharge is useful for deposition of graphene oxide from the gas phase because it can easily break most of the chemical bonds and overcome of the disadvantage of using high temperature in conventional chemical vapor deposition methods [28].

4. Conclusion

In this study, we present the electric and optical characteristics of CCP system that was constructed with the intention of using it to deposit graphene oxide at frequency 13.56 MHz. The system can run at wide range of pressures from 3.5 mbar to 1 bar using bare metallic copper electrode with power up to 150 W at constant gap 5 mm. The behaviour of glow discharge was observed by I−V waveform in all conditions. Electric characteristics like I−V wave form, the consumed power was calculated and found to be 40−50 % of input power, phase angle, impedance and Lissajous figures were recorded. ɣ mode was observed at all conditions. The existence of nitrogen second positive system, atomic and ionic argon emission lines, and atomic oxygen emission lines were found during discharge species identification. The exaction temperature was calculated using Boltzmann plot method and found to be the range 2.5 ev−3.5 ev depend on the pressure. Rotational (T_{rot}) and vibrational (T_{vib}) temperatures were demonstrated that the discharge system in current work is nonthermal plasma making it a good candidate to deposit different material especially carbon materials from the gas phase of the discharge when operated with a mixture of argon and methane gas or argon acetylene mixture.

Conflicts of interest

None declared.

Acknowledgments

We acknowledge Coaxial Power Systems Ltd England for supporting this work by fixing and maintaining the power supply for free.

References

[1] Bora B, Bhuyan H, Favre M, Wyndham E, Chuaqui H. Diagnostic of capacitively coupled radio frequency plasma by homogeneous discharge model. Phys Lett Sect A Gen At Solid State Phys [Internet] 2012;376(16):1356−9. Available from: https://doi.org/10.1016/j.physleta.2012.03.004.
[2] Schütze A, Jeong JY, Babayan SE, Park J, Selwyn GS, Hicks RF. The atmospheric-pressure plasma jet: a review and comparison to other plasma sources. IEEE Trans Plasma Sci 1998;26(6):1685−94.
[3] Li HP, Li G, Wang S, Le PS, Bao CY. Radio-frequency glow discharges of different gases using bare metallic electrodes at atmospheric pressure. IEEE Trans Plasma Sci 2008;36(4 PART 1):1418−9.
[4] Li SZ, Wu Q, Wang D, Uhm HS. Breakdown mechanism of an atmospheric-pressure radio-frequency capacitive argon discharge in parallel-plate bare metal electrodes. Phys Lett Sect A Gen At Solid State Phys 2011;375(3):598−600.
[5] Moon SY, Rhee JK, Kim DB, Gweon BM, Choe W. Capacitive discharge mode transition in moderate and atmospheric pressure. Curr Appl Phys 2009;9(1):274−7.
[6] Ahmad MA. Influence of electrodes area ratios and the discharge volume in RF capacitively coupled plasma. Iraqi J Phys 2013;11(20):1−8.
[7] Li HP, Sun WT, Wang HB, Li G, Bao CY. Electrical features of radio-frequency, atmospheric-pressure, bare-metallic-electrode glow discharges. Plasma Chem Plasma Process 2007;27(5):529−45.
[8] Adetayo A, Runsewe D. Synthesis and fabrication of graphene and graphene oxide: a review. Open J Compos Mater 2019;09(02):207−29.
[9] Gyun M, Hong D, Myoung H, Kim T, Ho J, Yoo J, et al. Sensors and actuators B: chemical highly sensitive NO_2 gas

sensor based on ozone treated graphene. Sensors Actuators B Chem [Internet] 2012;166−167(2):172−6. Available from: https://doi.org/10.1016/j.snb.2012.02.036.
[10] Liu Y, Chen Y. Synthesis of large scale graphene oxide using plasma enhanced chemical vapor deposition method and its application in humidity sensing. J Appl Phys [Internet] 2016;119(10):1−7. Available from: https://doi.org/10.1063/1.4942999.
[11] Alam K, Jo YY, Park CK, Cho H. Synthesis of graphene oxide using atmospheric plasma for prospective biological applications. Int J Nanomed 2020;15:5813−24.
[12] Abdelradi A, Samir A, Elakshar F, Garamoon A, ElSabbagh M. Characterization of atmospheric-pressure DC-glow discharge in contact with liquid with a miniature argon flow. Egypt J Chem 2022;65(1):99−106.
[13] Raizer YP, Shneider MN, Yatsenko NA. Radio-frequency Capacitive Discharges. 1st ed. Boca Raton: CRC Press; 1995.
[14] Li SZ, Wu Q, Yan W, Wang D, Uhm HS. Influence of oxygen traces on an atmospheric-pressure radio-frequency capacitive argon plasma discharge. Phys Plasma 2011;18(10).
[15] Kong CS. A general maximum power transfer theorem. IEEE Trans Educ 1995;38(3):296−8.
[16] Shi JJ, Deng XT, Hall R, Punnett JD, Kong MG. Three modes in a radio frequency atmospheric pressure glow discharge. J Appl Phys 2003;94(10):6303−10.
[17] Farouk T, Farouk B, Gutsol A, Fridman A. Atmospheric pressure radio frequency glow discharges in argon: effects of external matching circuit parameters. Plasma Source Sci Technol 2008;17(3).
[18] Laimer J, Störi H. Glow discharges observed in capacitive radio-frequency atmospheric-pressure plasma jets. Plasma Process Polym 2006;3(8):573−86.
[19] Moon SY, Rhee JK, Kim DB, Choe W. A, Γ and normal, abnormal glow discharge modes in radio-frequency capacitively coupled discharges at atmospheric pressure. Phys Plasma 2006;13(3):1−7.
[20] Li L, Nikiforov A, Britun N, Snyders R, Leys C. Emission and absorption spectroscopy study of Ar excited states in 13.56 MHz argon plasma operating at sub-atmospheric to atmospheric pressure. Spectrochim Acta − Part B At Spectrosc 2015;107:75−85.
[21] Országh J, Danko M, Ribar A, Matejc Š. Nitrogen second positive system studied by electron induced fluorescence. Nucl Instrum Methods Phys Res Sect B Interact Mater Atoms 2012;279:76−9.
[22] Guo QJ, Ni GH, Li L, Lin QF, Zhao P, Meng YD, et al. Characteristics of an atmospheric-pressure radio frequency-driven Ar/H_2 plasma discharge with copper wire in tube. Contrib Plasma Phys 2018;58(4):252−9.
[23] Ohno N, Razzak MA, Ukai H, Takamura S, Uesugi Y. Validity of electron temperature measurement by using boltzmann plot method in radio frequency inductive discharge in the atmospheric pressure range. Plasma Fusion Res 2006;1. 028−028.
[24] NIST Atomic Spectra Database Data [Internet]. Available from: http://physics.nist.gov.
[25] Mazhir SN, Khalaf MK, Taha SK, Mohsin HK. Measurement of plasma electron temperature and density by using different applied voltages and working pressures in a magnetron sputtering system. Int J Eng Technol 2018;7(3): 1177−80.
[26] Lempert WR, Adamovich IV, Sintsov S, Tabata K, Yamada S, Morita Y, et al. Experimental Study of Temperatures of Atmospheric-Pressure Nonequilibrium Ar/N_2 Plasma Jets and Poly (ethylene terephtalate) − Surface Processing. 2007.
[27] Abdelradi A, Samir A, Elakshar F, Garamoon A, ElSabbagh M. Optical characterization of stabilized atmospheric pressure pin to plate plasma source. Al-Azhar Bull Sci Sect B 2021;32(1-B):27−44.
[28] Morgan NN, ElSabbagh M. Hydrogen production from methane through pulsed DC plasma. Plasma Chem Plasma Process 2017;37(5):1375−92.